IEEE Access
Multidisciplinary | Rapid Review | Open Access Journal

Received 24 April 2024, accepted 5 June 2024, date of publication 11 June 2024, date of current version 19 June 2024.

Digital Object Identifier 10.1109/ACCESS.2024.3412684

RESEARCH ARTICLE

Design of Pinning Control Strategies of Different Neural Population Networks for Neuromodulation Research

CHENGXIA SUN[1], LIJUN GENG[1], HONGJU LIN[1], YUQUAN MA[1], XIAN LIU[2], AND JIANJIANG LI[3]

[1]Mechanical and Electrical Engineering College, Hebei Normal University of Science and Technology, Qinhuangdao 066004, China
[2]State Key Laboratory of Intelligent Rehabilitation and Neuromodulation of Hebei Province, Institute of Electrical Engineering, Yanshan University, Qinhuangdao 066004, China
[3]Tangshan Shangxinrongda Electronics Company Ltd., Tangshan 063504, China

Corresponding author: Xian Liu (liuxian@ysu.edu.cn)

This work was supported in part by the National Natural Science Foundation of China under Grant 62073278, Grant 61473245, and Grant 61004050; in part by the Natural Science Foundation of Hebei Province under Grant F2017203218 and Grant F2021203020; in part by Hebei Province Innovation Capability Improvement Plan Project under Grant 22567619H; and in part by the Science Research Foundation of Hebei Normal University of Science and Technology under Grant 2023YB022 and Grant 2023YB021.

ABSTRACT In order to comply with the development trend of the ''Brain Project'', China has listed the neural basis for explaining cognitive function as a core pillar, emphasizing the investment of resources and research capabilities into urgent social needs such as early diagnosis and intervention treatment of neurological and psychiatric diseases. The control scheme proposed on the basis of neural computational models can predict changes in brain dynamics induced by neurostimulation, which helps to develop more effective treatment plans for neurological and psychiatric diseases, while reducing the risk of brain damage and secondary injury that may result from direct animal experiments or clinical trials. The paper presents such a theoretical method for modulating brain dynamics based on the concept of pinning control from complex network control theory to suppress spikes generated by neural population networks affected by measurement noise. The main issues to be addressed of the work include: how to select driving nodes (the locations where need to exert neurostimulation) to better ensure the effectiveness of pinning strategies for neural population networks with different topologies? What are relationships among control gain, control energy, coupling strength and the number of driving nodes while ensuring the effectiveness of control strategies? To solve these problems, firstly, based on the Wendling-type neural population model, graph theory and complex network theory are applied to construct neural population networks with ''nearest-neighbor'', ''scale-free'' and ''small-world'' topologies, respectively. Then, different pinning control strategies are designed to modulate the brain dynamics simulated by the established network models according to the degree distribution, and better strategies are determined through simulation experiments. The local control adopts the output-feedback method based on the fuzzy regulator and cubature Kalman filter algorithm. Finally, the effects of coupling strength and number of driving nodes on control gain amplitude and control energy are studied using analytical and statistical methods. This work provides new ideas for the development of neuromodulation strategies in the treatment of neurological and psychiatric diseases, and is expected to play a potential role in future clinical applications.

INDEX TERMS Cubature Kalman filter algorithm, fuzzy regulator, neural population networks, neuromodulation research, pinning control.

I. INTRODUCTION

In terms of the progress of the global ''Brain Project'', developing prevention and treatment technologies for neurological and psychiatric diseases is one of the priority projects that

The associate editor coordinating the review of this manuscript and approving it for publication was Nasim Ullah.

should be considered in medical and health policies [1], [2]. Revealing the mechanisms underlying physiological functions such as cognition and behavior is a necessary foundation for understanding the causes of neurological and psychiatric diseases, and fully understanding the pathogenesis of neurological and psychiatric diseases can help formulate the most effective prevention and treatment plans for patients. Current research suggests that cognitive, behavioral and other abilities stem from rhythmic electrical activities, known as neural oscillations, triggered by large-scale neuronal interactions in the cerebral cortex [3], [4]. According to the frequency coverage range, neural oscillations are usually divided into delta (1-4Hz), theta (4-7Hz), alpha (8-12Hz), beta (13-30Hz) and gamma (30-100Hz) oscillation [5]. More and more experimental and clinical data supports the view that abnormal neural oscillations can transfer brain function from a physiological state to a pathological state, leading to neurological or psychiatric diseases [6]. For example, the theta oscillation of Alzheimer's patients is significantly enhanced during sleep [7]; The neural oscillations generated by the synchronous activity of patients' cortical neurons exhibit spikes during epileptic seizures [8]. Appropriate neural stimulation can normalize abnormal neural oscillations that cause neurological or psychiatric diseases, which plays an important role in promoting brain function recovery in patients and improving human mental health levels [9], [10], [11]. Given the significant individual differences in patients with neurological and psychiatric diseases, repeated experiments may be necessary to determine the optimal neural stimulation parameters, while direct animal or clinical trials may increase the risk of brain damage and secondary injury. The neural population model originated in the 1970s not only helps to study the mechanism of static neural oscillations generated by autonomous discharge of neurons in the cerebral cortex, but can also simulate the evolutionary mechanism of neural oscillations induced by neural stimulation [12], [13], [14]. David and Friston pointed out that neural population models can generate different neural oscillations in various physiological and pathological states by simply changing intrinsic parameters [15]. Karoly et al. tracked clinical data from 12 patients with focal epilepsy recorded by cortical electroencephalography during more than 3000 seizures by changing the parameters of the neural population model, providing a powerful method for further experimental research to generate verifiable hypotheses about the working principles of the brain [16]. Basu et al. used neural population models to simulate the evoked responses of human and non-human primates to cortical and subcortical stimuli, providing a theoretical basis for developing the optimal neural stimulation strategy based on the patient's specific situation and the rehabilitation goals to be achieved [14]. Therefore, making assumptions and predictions according to the changes in brain dynamics under external stimuli simulated by control schemes developed on the basis of neural population models can help form new theoretical achievements and guide the future development direction of ''Brain Project''.

At present, a series of important achievements have been made in the research of brain dynamics modulation based on neural population models. However, the research objects are generally rule models with simple topological structures, which are difficult to fully describe the intricately complex and highly variable nature of the brain. Schirner et al. pointed out that the human brain is an extremely complex dynamic network [17]. Specifically, a neuron cluster local area network that performs specific functions is composed of large-scale neurons with interactions, and further forms a ''network of networks'' through information exchange with other neuron cluster local area networks. As far back as the early 1990s, Felleman and Van Essen discovered a number of anatomical structural connectivity features by summarizing the layout of visually relevant regions in the mammalian cerebral cortex, which later proved to be compatible with the ''small-world'' characteristics [18]. With the development and advancement of neuroimaging technology, more and more studies have pointed out that there are functional connectivity relationships closely related to resting or task states in different brain regions. The Salvador team was the first to clarify that the resting state functional network of the human brain derived from functional magnetic resonance imaging (fMRI) data has ''small-world'' characteristics [19], [20]. Eguíluz et al. used fMRI technology to extract the functional networks of relevant brain regions in subjects performing on-off finger tapping tasks, and found that the distribution of functional connections was ''scale-free'' and had ''small-world'' characteristics [21]. After analyzing the electroencephalogram (EEG) data from subjects, Ferri et al. pointed out that the functional connections between brain regions that achieve slow-wave synchronization during sleep exhibit characteristics of the ''small-world'' network [22]. These brain functional networks that can be reverse deduced utilizing technologies such as EEG, Magnetoencephalogram (MEG), fMRI and local field potential (LFP) indicate that when mammals are in a physiological state, their brain functional connections have the dual characteristics of ''small-world'' and ''scale-free''. Constructing neural population networks with different topologies on the basis of existing neural population models is not only beneficial for a more comprehensive understanding of the seizure mechanisms of various neurological and psychiatric diseases, but also lays a necessary theoretical foundation for the development and improvement of clinical diagnosis and intervention treatment technologies for neurological and psychiatric diseases.

Since the 21st century, neuroscientists have put forward increasingly high demands for the accuracy of computational neural research with the rise of ''Brain Project'' in various countries. Therefore, for the brain dynamics modulation system with a more realistic neural population network as the controlled object, how to take advantage of existing feedback

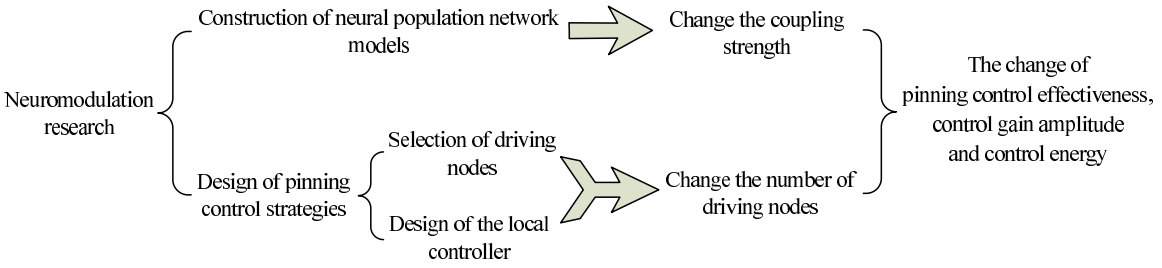

FIGURE 1. The issues that need to be addressed in the paper.

control schemes to ensure its economic effectiveness has become one of the urgent problems to be solved. Considering the diversity of brain regions involved in the occurrence of neurological and psychiatric diseases, as well as individual differences in patient symptoms, the choice of neural stimulation sites directly affects the effectiveness of the modulation system, which is of great significance for maximizing the therapeutic effect [23]. With the further cross-penetration between complex networks and control theory, the concept of pinning control provides ideas for improving treatment techniques for neurological and psychiatric diseases [24], [25]. Grigoriev et al. first clarified that pinning control is to exert feedback control on some nodes (known as driving nodes) in the network, and then ensures that the entire network generates the desired dynamic behavior through the ''virtual control'' between the coupling nodes [26]. Compared to the method of controlling all nodes, the idea of using local feedback control to constrain the behavior of the entire network has more theoretical and practical value, especially in the field of neuroscience which takes the brain as the research object, due to its advantages of lower resource consumption, flexible and versatile control approaches, simple and easy operation, etc. The selection of driving nodes is the primary issue to consider in the research of complex network control. Node degree is the simplest and most direct method to describe the network topology quantitatively [27]. Considering that the control ability of driving nodes is affected by the degree distribution of nodes in the network, the pinning control strategies derived on the basis of node degree mainly include random pinning, specific pinning, uniform distribution pinning, and centralized distribution pinning. The random pinning strategy is to randomly select several nodes in the network to exert external control, while the specific pinning strategy is to sequentially select several nodes with the largest or smallest degree in the network for control, and these strategies are suitable for irregular networks with inconsistent node degrees. The uniform distribution and centralized distribution pinning strategies adopt control methods that make the driving nodes uniformly or centrally distributed, respectively, and these strategies are suitable for regular networks with consistent node degrees. Liu et al. found that priority should be given to selecting nodes with larger degrees as driving nodes when the percentage of driving nodes in the network is relatively small, but it is more advantageous to choose nodes with smaller degrees as driving nodes when the percentage is relatively large [28]. Chen et al. confirmed that if the control gain and the coupling strength between nodes are large enough, a single controller can drive the output of the entire network to the desired trajectory [29]. However, this control method will greatly increase the control cost, and it is difficult to achieve in reality. In summary, in addition to selecting driving nodes, seeking a balance between coupling strength, the control gain and the number of driving nodes is also a fundamental and highly challenging issue in the design of pinning control schemes for different neural population networks.

For the sake of meeting the development needs of the ''Brain Project'', this paper aims to provide a more reasonable theoretical method for the neuromodulation research. Figure 1 states the issues that need to be addressed in the paper, and we carry out the following targeted work to solve these problems. Firstly, graph theory and complex network theory are used to establish neural population network models, such as ''nearest-neighbor'', ''scale-free'' and ''small-world'' networks, to simulate the neural oscillations recorded by techniques such as EEG, MEG, fMRI, and LFP. Then, considering the highly nonlinear and stochastic characteristics of neural population networks, as well as the potential impact of measurement noise on network outputs, we design an output-feedback control scheme based on the fuzzy regulator and cubature Kalman filter (CKF) algorithm to suppress the spikes produced by the driving nodes. The introduction of the fuzzy regulator in the control framework is to adaptively adjust the control gain matrix to better ensure the effectiveness of modulation. Further, select the driving nodes based on the degree distribution of nodes, and then the dynamics required for the entire network are generated through ''virtual control''. Specifically, the output modulation of the ''nearest-neighbor'' neural population network model is achieved through uniform and centralized distribution pinning strategies, while the output modulation of the ''scale-free'' and ''small-world'' neural network models is achieved through random and specific pinning strategies. Finally, some simulation examples are given to analyze the effectiveness of different pinning control

strategies for the established neural population networks, and the effects of coupling strength and the number of driving nodes on the effectiveness of control strategies as well as the control gain amplitude and control energy are summarized through analysis and statistical methods.

II. MATERIALS AND METHODS

A. CONSTRUCTION AND QUANTITATIVE DESCRIPTION METHODS OF NEURAL POPULATION NETWORKS

Wendling et al. have confirmed that more complex brain activities can be simulated by increasing the number of neural populations [30]. Constructing neural population networks with different topologies based on neural population models is more in line with the complex characteristics of the brain. The complex network theory based on graph theory holds that a concrete network can be abstracted into a graph composed of nodes and edges [31]. Thus, the brain functional network can be described as a graph composed of nodes representing neural populations and edges representing functional connectivity relationships [32]. The topological structure of neural population networks can be quantitatively described by node degree. The node degree is defined as the total number of edges directly connected to the node. The larger the degree, the more important the node is in the network. The average degree of a network is the average value of all node degrees. The larger the average degree, the tighter the connections between nodes.

1) THE CONSTRUCTION METHOD OF WS TYPE "SMALL-WORLD" NEURAL POPULATION NETWORK

According to the random reconnection process of the "small-world" network proposed by Watts and Strogatz [33], the construction of the "small-world" neural population network can be summarized into the following two steps. Firstly, establish a "nearest-neighbor" neural population network with N nodes, and connect each node to $K/2$ neighbor nodes on the left and right sides, where K should be even. Secondly, the edges of the "nearest-neighbor" network are randomly reconnected with the probability $P(0 < P < 1)$, ensuring that there is at most one edge between any two different nodes, and each node cannot be connected to itself. The transformation of the network between regularity and randomness can be closely monitored by changing the reconnection probability P. Figure 2 shows the random reconnection process from a "nearest-neighbor" regular network to a "small-world" network and then to a "random" network as the reconnection probability P increases when $N = 20$ and $K = 4$.

2) THE CONSTRUCTION METHOD OF BA TYPE "SCALE-FREE" NEURAL POPULATION NETWORK

Barabási and Albert first confirmed the existence of self-organization for characterizing large-scale features of complex networks, and they suggested that self-organizing large networks into "scale-free" states is an unpredictable feature of existing "random" networks [34]. The

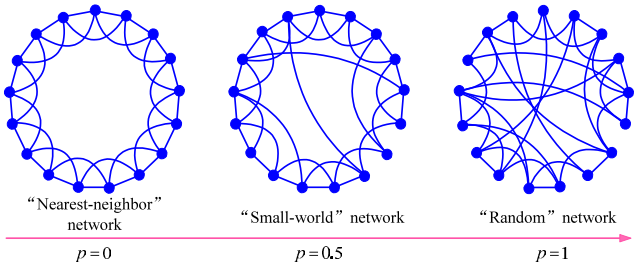

FIGURE 2. Random reconnection process for generating "small-world" and "random" networks with $N = 20$ and $K = 4$.

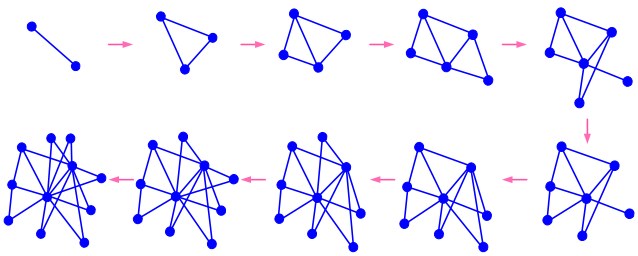

FIGURE 3. The formation process of the "scale-free" network.

"scale-free" nature of networks stems from two generation mechanisms, namely, continuously expanding the network by adding new nodes, and selectively connecting new nodes to existing nodes with larger degrees. Therefore, the construction process of the BA "scale-free" neural population network can be summarized into two steps. First, node addition process: Starting from a small number of nodes (m_0), a new node with m ($m \leq m_0$) edges is added at each time interval, and the new node is connected to m different existing nodes. Second, the optimal connection process: Connect the new node to node l with the probability of $\Pi(k_l) = k_l / \sum_{j=1}^{N} k_j$, where N represents the total number of existing nodes and k_l is the degree of node l. After t time intervals, the original neural population model evolves into a "scale-free" network with $t+m_0$ nodes and m_t edges. Figure 3 intuitively illustrates the formation process of a "scale-free" network with $m_0 = m = 2$.

3) MATHEMATICAL DESCRIPTION OF NEURAL POPULATION NETWORK MODELS

For the neural population network composed of N nodes, each node is a neural population described by a set of differential equations, with the form of [30]

$$\begin{cases} \dot{x}^l(t) = Ax^l(t) + Bf(Hx^l(t)) + B_1 p^l(t) + \delta \sum\limits_{\substack{m=1, \\ m \neq l}}^{N} Dx^m(t), \\ y^l(t) = Gx^l(t), \end{cases} \tag{1}$$

where $N \geq 2$ indicates the total number of populations, superscripts l ($l = 1, 2, \cdots, N$) and m ($m = 1, 2, \cdots, N$) denote the l-th and m-th populations, respectively. The endogenous stochastic or deterministic noise input $p^l(t)$

represents the average pulse density of afferent action potentials from adjacent or distant populations. The constant $\delta > 0$ denotes the coupling strength between populations. $x^l(t) = [x_1^l(t)\ x_2^l(t)\ \cdots\ x_8^l(t)]^T$ represents the state vector, in which $x_1^l(t)$, $x_3^l(t)$, $x_5^l(t)$, $x_7^l(t)$ are outputs of postsynaptic potential blocks, and $x_2^l(t), x_4^l(t), x_6^l(t), x_8^l(t)$ are their time derivatives, respectively. $y^l(t)$ is the postsynaptic membrane potential of the main neuron subset, which can be used to simulate the rhythmic electrical activity of cortical neural populations recorded by head-mounted or implantable electrodes. A, B, H, B_1, D, G are constant matrices with forms of

$$
\begin{aligned}
&A = \mathrm{diag}(A_1, \ldots, A_4),\\
&A_j = \begin{bmatrix} 0 & 1 \\ -\mu_j^2 & -2\mu_j \end{bmatrix}, \quad j = 1, 2, 3, 4,\\
&\mu_1 = \mu_2 = \frac{1}{\tau_e}, \quad \mu_3 = \frac{1}{\tau_i}, \ \mu_4 = \frac{1}{\tau_d},\\
&B = \begin{bmatrix} 0 & \frac{\theta_A}{\tau_e} & 0 & 0 & 0 & 0 & 0 & \frac{\theta_A}{\tau_d} \\ 0 & 0 & 0 & \frac{\theta_A}{\tau_e}C_2 & 0 & 0 & 0 & 0 \\ 0 & 0 & 0 & 0 & 0 & \frac{\theta_B}{\tau_i}C_4 & 0 & 0 \end{bmatrix}^T,\\
&H = \begin{bmatrix} H_1 \\ H_2 \\ H_3 \end{bmatrix} = \begin{bmatrix} 0 & 0 & 1 & 0 & -1 & 0 & 0 & 0 \\ C_1 & 0 & 0 & 0 & 0 & 0 & 0 & 0 \\ C_3 & 0 & 0 & 0 & 0 & 0 & 0 & 0 \end{bmatrix},\\
&B_1 = \begin{bmatrix} 0 & 0 & 0 & \frac{\theta_A}{\tau_e} & 0 & 0 & 0 & 0 \end{bmatrix}^T,\\
&D = \begin{bmatrix} \mathbb{O}_{3\times 6} & \mathbb{O}_{3\times 1} & \mathbb{O}_{3\times 1} \\ \mathbb{O}_{1\times 6} & \frac{\theta_A}{\tau_e}\gamma^{lm} & 0 \\ \mathbb{O}_{4\times 6} & \mathbb{O}_{4\times 1} & \mathbb{O}_{4\times 1} \end{bmatrix},\\
&G = \begin{bmatrix} 0 & 0 & 1 & 0 & -1 & 0 & 0 & 0 \end{bmatrix},
\end{aligned}
$$

where $\mathbb{O}_{m\times n}$ represents the zero matrix of $m \times n$ dimension. γ^{lm} determines the topological structure of networks. If there is a functional connection that characterizes the information exchange between population l and population m, then γ^{lm}=1; otherwise γ^{lm}=0. θ_A and θ_B are excitatory and inhibitory parameters, which determine the maximum amplitudes of excitatory and inhibitory postsynaptic potentials, respectively. τ_e and τ_i are lumped parameters linked to the average time constant of the passive membrane and all other spatially distributed delays in the dendritic network; τ_d is the average time delay related to functional connections among populations. The connectivity constants $C_1 - C_4$ represent the average number of synaptic contacts from axons of main cells to interneurons and from axons of interneurons to main cells. It should be noted that the local parameters θ_A, θ_B, τ_e, τ_i, τ_d, $C_1 - C_4$ depend on the population l and may vary from one population to another. For the sake of simplicity, the superscript l is not added to these parameters. The continuous

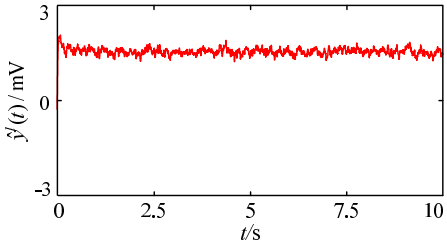

FIGURE 4. Alpha-like oscillations.

nonlinear vector function $f(Hx^l(t))$ has the form

$$
f(Hx^l(t)) = \begin{bmatrix} S(H_1x^l(t)) \\ S(H_2x^l(t)) \\ S(H_3x^l(t)) \end{bmatrix}, \tag{2}
$$

where the static nonlinear function $S(H_jx^l(t))$ has the sigmoid form

$$
S(H_jx^l(t)) = \frac{2e_0}{1 + e^{r(v_0 - H_jx^l(t))}}, \quad j = 1, 2, 3, \tag{3}
$$

where e_0 characterizes the maximum firing rate of the neural population, v_0 is the postsynaptic potential when the firing rate achieves 50%, and r indicates the bending degree of the sigmoid function.

It is known that the neural population model will produce alpha-like oscillations as shown in Figure 4, when all parameters are set to standard values [33]

$$
\begin{aligned}
&\theta_A = 3.25mV, \quad \theta_B = 22mV, \ \mu_1 = 101, \sigma_1 = 35,\\
&\tau_e = 0.0108s, \quad \tau_i = 0.02s, \ \tau_d = 0.0303s,\\
&C_1 = 135, \quad C_2 = 108, \ C_3 = C_4 = 33.75,\\
&e_0 = 2.5s^{-1}, \quad v_0 = 6mV, \ r = 0.56mV^{-1}
\end{aligned} \tag{4}
$$

where μ_1 and σ_1 are the average and standard deviation of the endogenous input $p^l(t)$ simulated by Gaussian white noise, respectively. Existing studies have shown that most neurological and psychiatric diseases result from internal instability caused by the disruption of the excitation/inhibition balance in the brain system. For example, when one or some brain regions are over-excited and beyond the self-adjustment scope of the brain system, they become hyper-excitatory regions, and abnormal neural oscillations generated by these regions spread to other regions under the action of functional connections, leading to the onset of neurological and psychiatric diseases [35]. That is to say, hyper-excitatory brain regions may be the source of lesions of neurological and psychiatric diseases. Therefore, a common method to simulate the onset mechanism of neurological and psychiatric diseases is to increase the excitatory parameters of neural populations to make them become hyper-excitatory neural populations [36].

For the convenience of computer implementation, it is commonly necessary to discretize the continuous systems in modern control system theory research. Typical continuous nonlinear systems, such as the neural population network

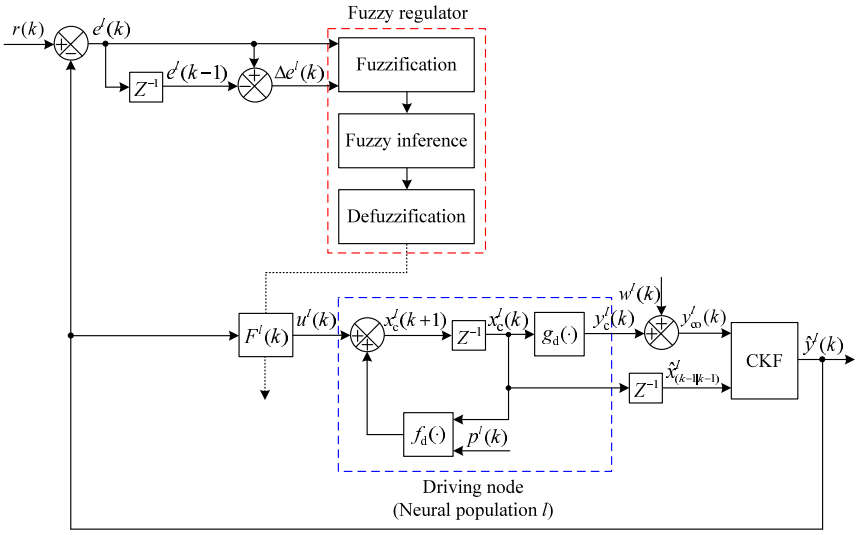

FIGURE 5. Structure diagram of dynamic modulation system of driving node based on the fuzzy regulator and CKF algorithm.

model (1), can be discretized as

$$\begin{cases} x^l(k) = f_d\left(x^l(k-1), p^l(k-1)\right) \\ y^l(k) = g_d\left(x^l(k)\right) \end{cases} \tag{5}$$

where k indicates the sampling sequence number; $f_d(\cdot)$ and $g_d(\cdot)$ are functions that can be derived from equation (1).

B. DESIGN OF THE CONTROL SCHEME FOR NEUROMODULATION

The aim of the paper is to transform high-amplitude spikes that characterize the onset of neurological or psychiatric diseases into alpha-like oscillations that reflect normal brain activity through modulating the brain dynamics modeled by neural population networks. It is often unnecessary to control all populations for neural population networks because this approach can easily lead to system instability due to excessive control. According to the concepts related to network control, it can be clearly stated at the theoretical level that for a connected neural population network, as long as the coupling strength between populations and the control gain are appropriate, the modulation target can definitely be achieved by controlling partial nodes in the network. Given that the distribution of node degrees in the network can affect the control ability of driving nodes, it is necessary to adopt different pinning control strategies based on the characteristics of the degree distribution of different networks to modulate the brain dynamics simulated by neural population networks. For the "nearest-neighbor" neural population network with consistent node degrees, we adopt uniform distribution and centralized distribution pinning control strategies. For "small-world" and "scale-free" neural population networks with inconsistent node degrees, we adopt random and specific pinning control strategies. Considering that the output of neural population networks may be affected by measurement noise, we design a feedback control scheme based on the CKF algorithm to modulate the dynamics of driving nodes, and introduce the fuzzy regulator to adaptively adjust the control gain to ensure the modulation effect. Then through the action of "virtual control", the entire network generates the desired dynamic behavior. The basic structural framework of the local control system is shown in Figure 5, where $p^l(k)$ represents the known endogenous noise input at the k-th sampling sequence; $r(k)$ and $y_c^l(k)$ are the expected and controlled outputs of the driving node, respectively; $y_{co}^l(k)$ is the measurement controlled output affected by measurement noise $w^l(k)$; $\hat{y}^l(k)$ indicates the estimated output obtained utilizing the CKF algorithm; control error $e^l(k) = r(k) - \hat{y}^l(k)$; $\Delta e^l(k)$ represents the rate of change in the control error; $x_c^l(k)$ is the controlled state vector; $\hat{x}^l_{(k-1|k-1)}$ indicates the posterior state estimation vector generated by the $(k-1)$-th iteration of the CKF algorithm; $F^l(k)$ denotes the control gain vector, and its general form is

$$F^l(k) = \left[0\ 0\ 0\ \lambda^l(k)\ 0\ 0\ 0\ 0\right]^T \tag{6}$$

where the control gain $\lambda^l(k)$ is a negative constant, but when the neural population l is not the driving node $\lambda^l(k) = 0$; the external control input vector $u^l(k) = F^l(k)\hat{y}^l(k)$; Z^{-1} represents time delay.

Each iteration process in which the estimated value constantly approximates the true value contains two time scales: a prior and a posterior, when take advantage of the CKF algorithm to estimate the output of a nonlinear system. Between these two time scales, there is a transformation process in which the posterior estimated values are obtained by correcting the prior estimated values, and the posterior estimate results obtained from each iteration are used to predict the prior knowledge of the next iteration [37]. Assuming that the posterior state estimation vector $\hat{x}^l_{(k-1|k-1)}$

and the posterior error covariance matrix $P^l_{(k-1|k-1)}$ at the sampling time point $k-1$ are known, and each component of the measurement noise follows a Gaussian distribution with zero mean and σ variance, then the mathematical expressions for estimating the k-th complete iteration of the output of the driving node using the CKF algorithm are as follows (the superscript l is not added to relevant parameters for simplicity):

1) Prediction process

$$\begin{aligned}
\chi_{(k-1)} &= Chol\left(P_{(k-1|k-1)}\right) \\
\varphi_i &= \chi_{(k-1)}\zeta_i + \hat{x}_{(k-1|k-1)},\ i = 1, 2, \ldots, 2n_x \\
\hat{x}_{(k|k-1)} &= \frac{1}{2n_x}\sum_{i=1}^{2n_x} f_d(\varphi_i) \\
P_{(k|k-1)} &= \frac{1}{2n_x}\sum_{i=1}^{2n_x} f_d(\varphi_i) f_d^T(\varphi_i) - \hat{x}_{(k|k-1)}\hat{x}^T_{(k|k-1)}
\end{aligned} \tag{7}$$

where n_x is the dimension of the state vector, then $n_x = 8$; $\chi_{(k-1)}$ is the Cholesky decomposition factor of the posterior error covariance matrix $P_{(k-1|k-1)}$, and $Chol(\cdot)$ represents the Cholesky decomposition function; φ_i is the cubature point, $\hat{x}_{(k|k-1)}$ and $P_{(k|k-1)}$ represent the prior state estimation vector and prior error covariance matrix at the sampling time point k, respectively; ζ_i is a standard orthogonal vector group whose elements are usually represented as

$$\zeta_i = \begin{cases} \sqrt{n_x}[I_{n_x}]_i, & i = 1, 2, \cdots, n_x \\ -\sqrt{n_x}[I_{n_x}]_i, & i = n_x+1, n_x+2, \cdots, 2n_x \end{cases}$$

where $[I_{n_x}]_i$ is the i-th column vector of the $n_x \times n_x$ dimensional identity matrix I_{n_x}. 2) Correction process

$$\begin{aligned}
\chi_{(k)} &= Chol\left(P_{(k|k-1)}\right) \\
\tilde{\varphi}_i &= \chi_{(k)}\zeta_i + \hat{x}_{(k|k-1)} \\
\hat{y}_{(k|k-1)} &= \frac{1}{2n_x}\sum_{i=1}^{2n_x} g_d(\tilde{\varphi}_i) \\
P_{xy} &= \frac{1}{2n_x}\sum_{i=1}^{2n_x} \tilde{\varphi}_i g_d^T(\tilde{\varphi}_i) - \hat{x}_{(k|k-1)}\hat{y}^T_{(k|k-1)} \\
P_{yy} &= \frac{1}{2n_x}\sum_{i=1}^{2n_x} g_d(\tilde{\varphi}_i) g_d^T(\tilde{\varphi}_i) - \hat{y}_{(k|k-1)}\hat{y}^T_{(k|k-1)} + \sigma \\
K &= P_{xy}P_{yy}^{-1} \\
\hat{x}_{(k|k)} &= \hat{x}_{(k|k-1)} + K\left(y_{co}(k) - \hat{y}_{(k|k-1)}\right) \\
P_{(k|k)} &= P_{(k|k-1)} - KP_{yy}K^T \\
\hat{y}_{(k|k)} &= g\left(\hat{x}_{(k|k)}\right)
\end{aligned} \tag{8}$$

where $\hat{y}_{(k|k-1)}$ is the prior output estimation vector at the sampling time point k; P_{xy} and P_{yy} represent the cross-covariance matrix and auto-covariance matrix, respectively; K is the Kalman filter gain matrix; $\hat{x}_{(k|k)}$, $P_{(k|k)}$ and $\hat{y}_{(k|k)}$ denote the posterior state estimation vector, posterior error covariance matrix and posterior output estimation vector at the sampling time point k, respectively, where $\hat{x}_{(k|k)}$ and $P_{(k|k)}$ are used for the $(k+1)$-th iteration operation.

TABLE 1. Fuzzy control rules.

$U(k)$ \ $\Delta e(k)$ / $e(k)$	NB	NM	NS	ZE	PS	PM	PB
NB	PB	PB	PM	PM	PS	ZE	ZE
NM	PB	PB	PM	PS	PS	ZE	NS
NS	PM	PM	PM	PS	ZE	NS	NS
ZE	PM	PM	PS	ZE	NS	NM	NM
PS	PS	PS	ZE	NS	NS	NM	NM
PM	PS	ZE	NS	NM	NM	NM	NB
PB	ZE	ZE	NM	NM	NM	NB	NB

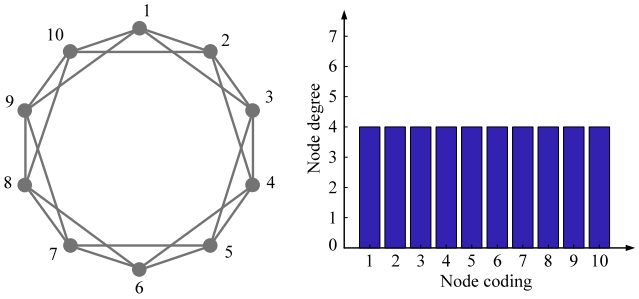

(a) Structural topology (b) Bar chart of node degree distribution

FIGURE 6. The "nearest-neighbor" network with 10 neural populations and its quantitative description.

The process of using the fuzzy controller to adaptively tune the control gain vector $F^l(k)$ in Figure 5 can be roughly summarized as follows (the superscript l is also not added to relevant parameters for simplicity):

1) Define a fuzzy set {NB, NM, NS, ZE, PS, PM, PB} in the fuzzy domain for fuzzification, where the subset "NB" means negative large, "NM" means negative middle, "NS" means negative small, "ZE" means zero, "PS" means positive small, "PM" means positive middle, "PB" means positive large, and the most commonly used triangular membership function is selected as the membership function of the fuzzy subsets;
2) Perform fuzzy processing on the control error $e(k)$ and error change rate $\Delta e(k)$, and use the obtained quantitative data as the input for the fuzzy regulator;
3) Perform fuzzy logic reasoning according to fuzzy rules. Table 1 presents 49 fuzzy control rules in the decision-making process, where $U(k)$ is the fuzzy output variable related to the control gain vector $F(k)$. The fuzzy reasoning method adopts the classical Mamdani minimax reasoning method;
4) The centroid method is used to defuzzify the fuzzy values obtained from inference into the control gain vector of the system.

C. THE PERFORMANCE METRIC FOR MEASURING THE CONTROL COST

Professors Wang and Chen pointed out that effectiveness is a fundamental issue for pining control referring to how

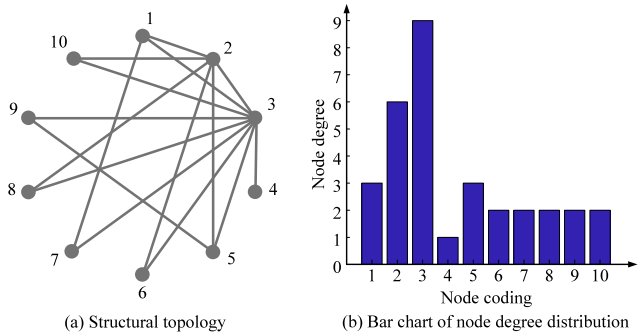

(a) Structural topology (b) Bar chart of node degree distribution

FIGURE 7. The "scale-free" network with 10 neural populations and its quantitative description.

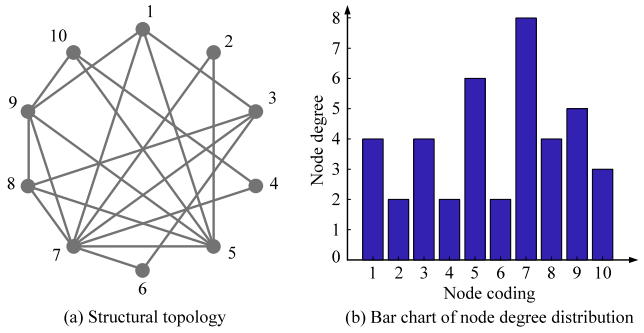

(a) Structural topology (b) Bar chart of node degree distribution

FIGURE 8. The "small-world" network with 10 neural populations and its quantitative description.

to select the driving nodes of networks to ensure that the control goal can be achieved with lower control cost [38]. The consumed control energy can generally be used as a performance metric to measure the cost of pinning control [39]. In order to quantify the energy consumption of the control process, we define the total control energy E_n required to achieve the modulation goal of brain dynamics as

$$E_n = \sum_{l=1}^{N} \sum_{k=1}^{M} \left(u^l(k)\right)^T u^l(k) \tag{9}$$

where M represents the total number of sampling times. The physical meaning of this expression is that the energy consumption is directly proportional to the size of the control signal [40].

III. RESULTS

A. CONSTRUCTION OF "NEAREST-NEIGHBOR", "SMALL-WORLD" AND "SCALE-FREE" NEURAL POPULATION NETWORKS

We construct "nearest-neighbor", "small-world" and "scale-free" neural population networks with 10 nodes respectively by using the methods mentioned in Subsection A of Section II. Each node in the network is a neural population described by the nonlinear ordinary differential equation system (1), and the edge represents the undirected connection relationship between the neural populations. The values of even K and reconnection probability P in the "nearest-neighbor" neural population network are 4 and 0. The values of K and P in the "small-world" neural population network are 4 and 0.8. The values of initial number of nodes m_0, number of new nodes m and reconnection probability $\Pi(k_l)$ in the "scale-free" neural population network are 3, 2 and 0.8. It should be emphasized that the network parameters in the paper are strictly selected according to the relevant requirements, which can ensure the relevant characteristics of "small-world" and "scale-free" networks. The topological structure and quantitative description of the constructed networks are shown in Figures 5, 6 and 7, respectively.

B. ANALYSIS OF THE EFFECTIVENESS OF PINNING STRATEGIES

The uniform distribution and centralized distribution pinning control strategies are adopted to modulate the brain dynamics simulated by the "nearest-neighbor" neural population network shown in Figure 6. The random and specific pinning control strategies are adopted to modulate the brain dynamics simulated by "small-world" and "scale-free" neural population networks shown in Figures 7 and 8, and the specific pinning strategy here is to sequentially select the node with the largest degree in the network for control. The dynamic modulation system diagram of the driving node based on the fuzzy regulator and CKF algorithm is shown in Figure 5. The paper will use Matlab software for numerical simulation analysis. In each of the simulations described below, equation (1) is numerically solved using the fourth-order Runge-Kutta method.

Assuming that the measurement noise is simulated by Gaussian distributed noise with the mean of $\mu_1 = 0$ and standard deviation of $\sigma_1 = 2$. In the neural population network shown as Figures 6, 7 and 8, except for the excitatory parameter of the population 1, which is a non-standard value of 3.4mV, all other local parameters are set to standard values shown in equation (4). The simulation time is 10s, and the time step is set to 0.001. The initial value of the state vector in neural population networks can be arbitrarily selected. In order to generate reference data, the measured output vector $y_o(k) = \left[y_o^1(k)\ y_o^2(k) \cdots y_o^{10}(k)\right]^T$ of different networks at each sampling time point are recorded, and then the variation curves of each component over time are plotted separately. At the same time, record the controlled state vectors and measurement controlled output vectors of different networks at each sampling time point, and the obtained $(k-1)$-th controlled state vector is re-input into the CKF algorithm as the posterior corrected state vector $\hat{x}_{(k-1|k-1)}$ for the k-th iteration. After the k-th iteration of the CKF algorithm, the output vector at the sampling time point k is $\hat{y}(k) = \left[\hat{y}^1(k)\ \hat{y}^2(k) \cdots \hat{y}^{10}(k)\right]^T$. Record the estimated output vectors of different networks at the end of each iteration, and then plot the variation curves of each component over time.

There are two points that need to be clarified in advance: Firstly, existing studies have shown that the hyper-excitatory neural populations in networks must serve as driving nodes;

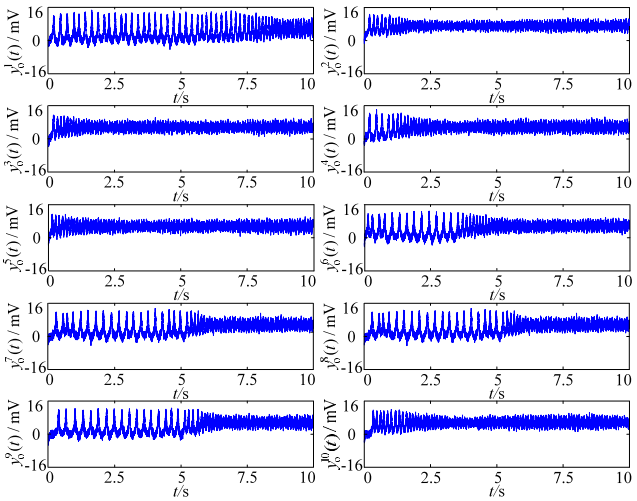

FIGURE 9. Output of the "nearest-neighbor" neural population network under the influence of measurement noise.

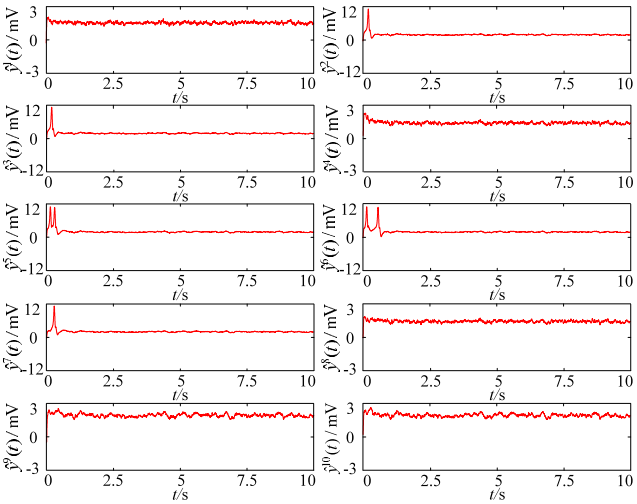

FIGURE 10. Modulation results of the first uniform distribution pinning strategy (1,4,8 are driving nodes).

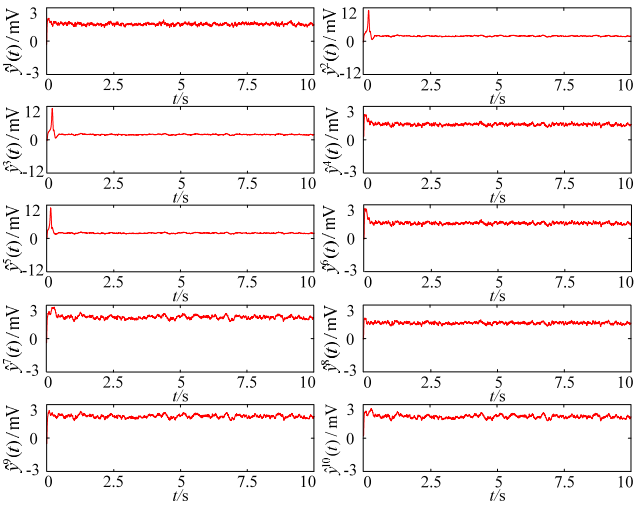

FIGURE 11. Modulation results of the second uniform distribution pinning strategy (1,4,6,8 are driving nodes).

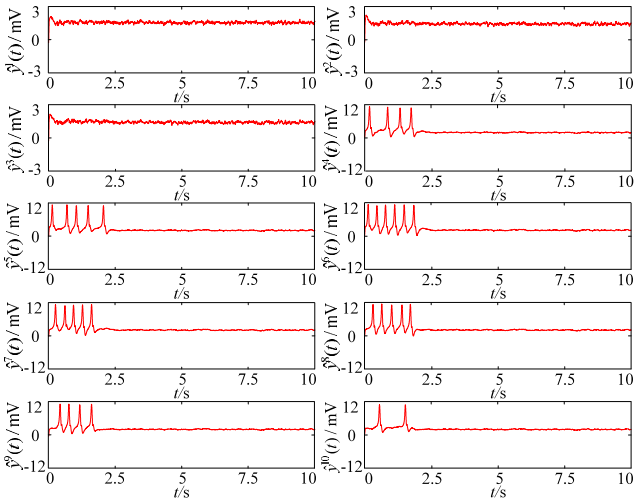

FIGURE 12. Modulation results of the first centralized distribution pinning strategy (1,2,3 are driving nodes).

Secondly, setting too many driving nodes may cause the system instability due to excessive control, and at the same time, the work requires that the number of driving nodes should be less than half of the total number of nodes in the network due to considerations such as ease of operation in clinical practice.

1) ANALYSIS OF THE EFFECTIVENESS OF PINNING STRATEGIES IN THE "NEAREST-NEIGHBOR" NEURAL POPULATION NETWORK

When the coupling strength between neural populations is 40, the outputs of the "nearest-neighbor" network shown in Figure 6 are shown in Figure 9 under the influence of measurement noise. It can be seen that if control measures are not taken, the spikes generated by the hyper-excitatory neural population 1 will propagate to the remaining 9 nodes of the "nearest-neighbor" neural population network under the coupling action. We propose two uniform distribution pinning strategies and two centralized distribution pinning strategies to modulate the brain dynamics simulated by the "nearest-neighbor" network to suppress the spikes in Figure 9. The first uniform distribution pinning strategy is to make the feedback control based on the fuzzy regulator and CKF algorithm act on nodes 1, 4 and 8, respectively, and the modulation results are shown in Figure 10. The second uniform distribution pinning strategy is to select neural populations 1, 4, 6 and 8 as the driving nodes, and the modulation results are shown in Figure 11. It is not difficult to see from the figures that both strategies can quickly drive the spikes generated by the "nearest-neighbor" neural population network to the expected alpha-like oscillations. The first centralized distribution pinning strategy is to make the feedback control based on the fuzzy regulator and CKF algorithm act on nodes 1, 2 and 3, respectively, and

TABLE 2. Statistical data of the uniform distribution pinning control strategies.

Driving node set	Coupling strength	Control gain amplitude ("-" indicates negative feedback)	Control energy (mV)
{1,4,8}	40	$\lambda_1 = -13.68, \lambda_4 = -13.68, \lambda_8 = -10.19$	6.7821×10^5
{1,4,6,8}	40	$\lambda_1 = -13.68, \lambda_4 = -12.51, \lambda_6 = -8.51, \lambda_8 = -8.56$	7.8454×10^5
	43	$\lambda_1 = -13.68, \lambda_4 = -13.67, \lambda_6 = -10.56, \lambda_8 = -11.08$	8.6148×10^5

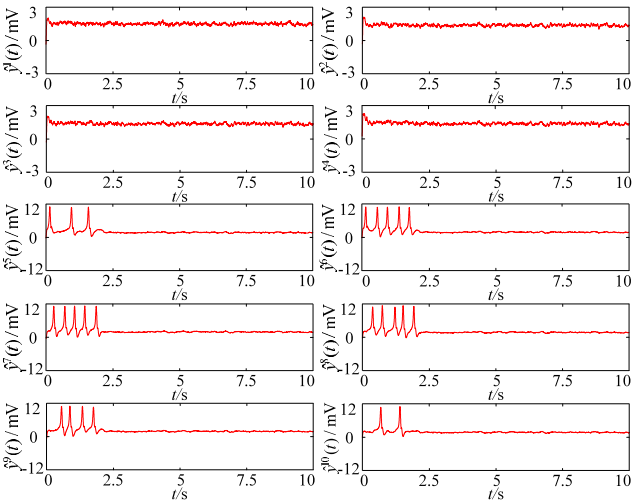

FIGURE 13. Modulation results of the second centralized distribution pinning strategy (1,2,3,4 are driving nodes).

the modulation result is shown in Figure 12. The second centralized distribution pinning strategy is to select neural populations 1, 2, 3 and 4 as the driving nodes, and the modulation results are shown in Figure 13. According to these two figures, it can be seen that except the spikes generated by the driving nodes that can be quickly suppressed, the spikes generated by the other nodes require a longer adjustment time to be driven to the expected alpha-like oscillations.The above results indicate that the adjustment time required for achieving the modulation target using the uniform distribution pinning strategy is obviously shorter than that of the centralized distribution pinning strategy. Therefore, the uniform distribution pinning strategy has significant advantages over the centralized distribution pinning strategy when modulating the brain dynamics simulated by the ''nearest-neighbor'' neural population network. We will then use the performance metric of the control cost to analyze the effectiveness of the more advantageous uniform distribution pinning strategy.

Table 2 presents statistical data for analyzing the effectiveness of the two proposed uniform distribution pinning strategies, where the values of control energy are calculated based on equation (9). It is not difficult to see from the table that: Firstly, when the coupling strength between neural populations is 40, the second strategy requires more control energy to achieve the modulation target compared with the first uniform distribution pinning strategy, and the control gain amplitudes required by driving nodes is smaller except that the control gain amplitude of the hyper-excitatory node remains unchanged; Secondly, for the second uniform distribution pinning strategy, with the increase of the coupling strength, the control energy required to achieve the modulation target increases, and the control gain amplitudes required by the driving nodes increase except that the control gain amplitude of the hyper-excitatory node remains unchanged. These results indicate that the coupling strength and the number of driving nodes can affect the effectiveness of the uniform distribution pinning strategy for the ''nearest-neighbor'' neural population network.

To sum up, the uniform distribution pinning strategy based on the fuzzy regulator and CKF algorithm has significant advantages over the centralized distribution pinning strategy for the ''nearest-neighbor'' neural population network whose output is affected by measurement noise. The statistical results further indicate that the coupling strength between neural populations and the number of driving nodes can affect the effectiveness of the uniform distribution pinning strategy. In general, for the ''nearest-neighbor'' neural population network with a certain coupling strength, the uniform distribution pinning strategy with fewer driving nodes can better ensure the effectiveness when the control energy is required to be as small as possible; But when the feedback control gain amplitudes of the driving nodes (except for the hyper-excitatory node) are required to be as small as possible, the uniform distribution pinning strategy with more driving nodes can better ensure the effectiveness. For a uniform distribution pinning strategy with a certain number of driving nodes, a smaller coupling strength between neural populations can better ensure its effectiveness, because the smaller the coupling strength, the less control energy and smaller control gain amplitudes required to achieve the modulation target.

2) ANALYSIS OF THE EFFECTIVENESS OF PINNING STRATEGIES IN THE ''SCALE-FREE'' NEURAL POPULATION NETWORK

When the coupling strength between neural populations is 40, the output of the ''scale-free'' network shown in Figure 7 is shown in Figure 14 under the influence of measurement noise. It can be seen that if control measures are not taken, the spikes generated by the hyper-excitatory neural population 1 will propagate to the remaining 9 nodes of the ''scale-free'' neural population network under the coupling action. We propose two specific pinning strategies and two random pinning strategies to modulate the brain dynamics simulated by the ''scale-free'' network to suppress the spikes in Figure 14. The first specific pinning strategy is to make the feedback control based on the fuzzy regulator and CKF

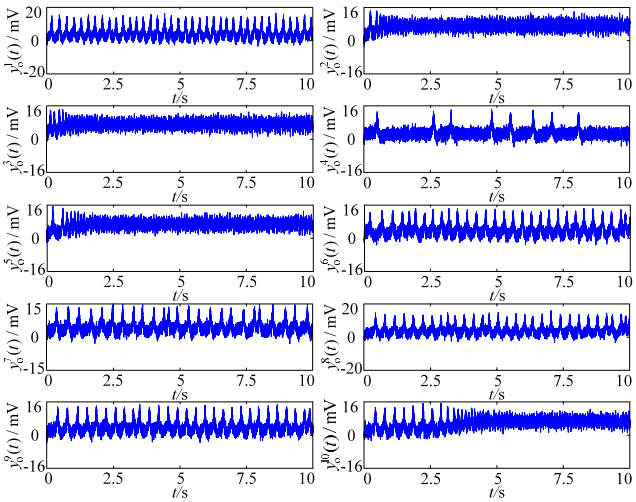

FIGURE 14. Output of the "scale-free" neural population network under the influence of measurement noise.

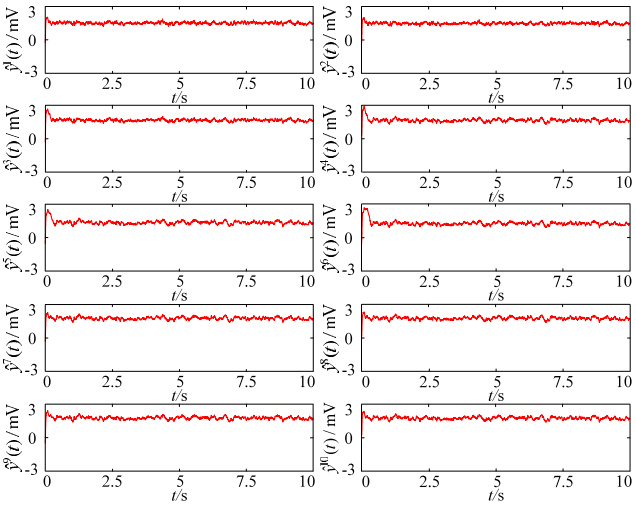

FIGURE 15. Modulation results of the first specific pinning strategy (1,3 are driving nodes).

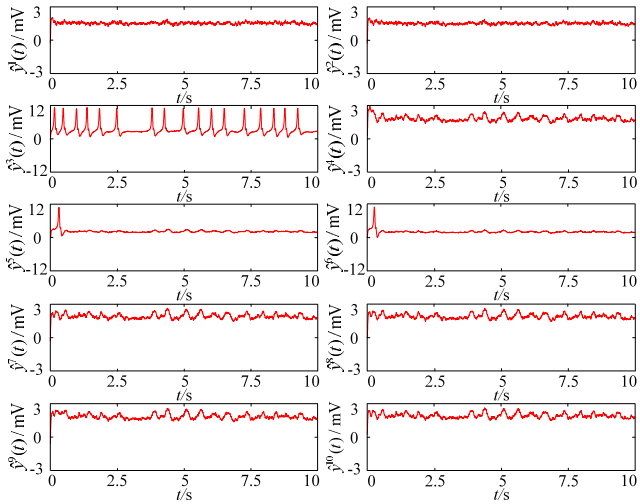

FIGURE 16. Modulation results of the first random pinning strategy (1,2 are driving nodes).

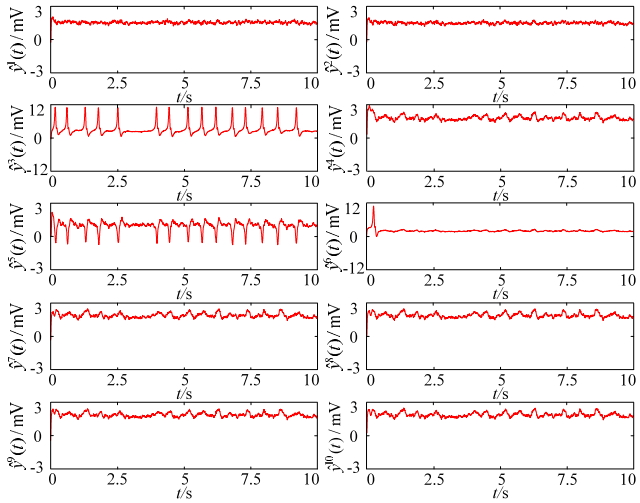

FIGURE 17. Modulation results of the second random pinning strategy (1,2,5 are driving nodes).

algorithm act on the hyper-excitatory neural population 1 and the node 3 with the highest degree, and the modulation results are shown in Figure 15. The second specific pinning strategy is to first apply feedback control to the hyper-excitatory neural population 1, and then sequentially select nodes 3 and 2 with the highest degree as the driving nodes. The modulation results are similar to which shown in Figure 15, so it is not repeated. It is not difficult to see from the figures that both strategies can quickly drive the spikes generated by the ''scale-free'' neural population network to the expected alpha-like oscillations. The first random pinning strategy is to make the feedback control based on the fuzzy regulator and CKF algorithm act on nodes 1 and 2, respectively, and the modulation results are shown in Figure 16. According to the figure, it can be seen that the 3-rd neural population in the ''scale-free'' network still continuously generates spikes, indicating that this control strategy cannot achieve the modulation target. The second random pinning strategy not only applies feedback control to the hyper-excitatory neural population 1, but also randomly selects populations 2 and 5 as the driving nodes, and the modulation results are shown in Figure 17.According to the figure, it can be seen that the 3-rd and 5-th neural populations in the ''scale-free'' network still continuously generate spikes, indicating that this control strategy is also unable to achieve the modulation target. In addition, we find that when the number of driving nodes is 2 or 3, only the specific pinning strategy can make the ''scale-free'' neural population network produce the expected dynamic behavior through a large number of simulation examples. The above results indicate that the specific pinning strategy has significant advantages over the random pinning strategy when modulating the brain dynamics simulated by the ''scale-free'' neural population network. We will then use the performance metric of the control cost to analyze

TABLE 3. Statistical data of the specific pinning control strategies.

Driving node set	Coupling strength	Control gain amplitude ("-" indicates negative feedback)	Control energy (mV)
{1,3}	40	$\lambda_1 = -13.53, \lambda_3 = -11.38$	6.2985×10^5
	56	$\lambda_1 = -13.68, \lambda_3 = -13.68$	1.0412×10^6
{1,2,3}	40	$\lambda_1 = -13.64, \lambda_2 = -13.66, \lambda_3 = -13.67$	7.7126×10^5
	61	$\lambda_1 = -13.68, \lambda_2 = -13.68, \lambda_3 = -13.68$	1.4372×10^6

the effectiveness of the more advantageous specific pinning strategy.

Table 3 presents statistical data for analyzing the effectiveness of the two proposed specific pinning strategies, where the values of control energy are calculated based on equation (9). It is not difficult to see from the table that: Firstly, when the coupling strength between neural populations is 40, the second strategy requires more control energy to achieve the modulation target compared to the first specific pinning strategy, and the control gain amplitudes required by driving nodes are relatively large; Secondly, for the first specific pinning strategy, with the increase of the coupling strength, the control energy required to achieve the modulation target increases, and the control gain amplitudes required by the driving nodes increase. These results indicate that the coupling strength and the number of driving nodes can affect the effectiveness of the specific pinning strategy for the ''scale-free'' neural population network.

To sum up, the specific pinning strategy based on the fuzzy regulator and CKF algorithm has significant advantages over the random pinning strategy for the ''scale-free'' neural population network whose output is affected by measurement noise. The statistical results further indicate that the coupling strength between neural populations and the number of driving nodes can affect the effectiveness of the specific pinning strategy. In general, for the ''scale-free'' neural population network with a certain coupling strength, the specific pinning strategy with fewer driving nodes can better ensure the effectiveness, because the less control energy and smaller control gain amplitudes are required to achieve the modulation target when the number of driving nodes is small. This phenomenon may be caused by excessive control due to the increase in the number of driving nodes. For a specific pinning strategy with a certain number of driving nodes, a smaller coupling strength between neural populations can better ensure its effectiveness, because the smaller the coupling strength, the less control energy and smaller control gain amplitudes required to achieve the modulation target.

3) ANALYSIS OF THE EFFECTIVENESS OF PINNING STRATEGIES IN THE ''SMALL-WORLD'' NEURAL POPULATION NETWORK

When the coupling strength between neural populations is 40, the output of the ''small-world'' network shown in Figure 8 is shown in Figure 18 under the influence of measurement noise. It can be seen that if no control measures are taken, the spikes generated by the hyper-excitatory neural

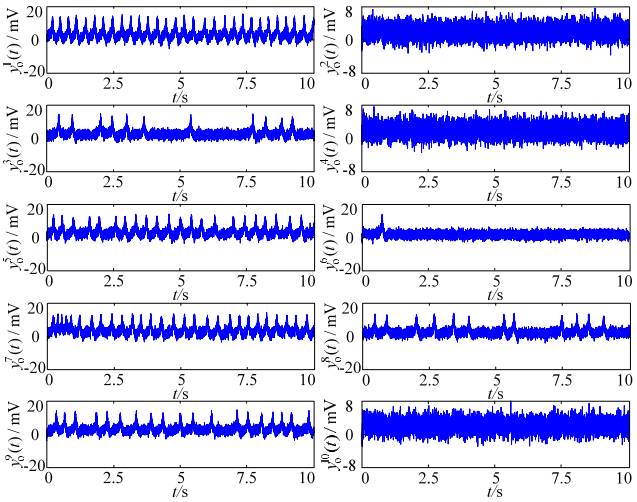

FIGURE 18. Output of the ''small-world'' neural population network under the influence of measurement noise.

population 1 will propagate to the remaining 9 nodes of the ''small-world'' neural population network under the coupling action. We propose two specific pinning strategies and three random pinning strategies to modulate the brain dynamics simulated by the ''small-world'' network to suppress the spikes in Figure 18. The first specific pinning strategy is to make the feedback control based on the fuzzy regulator and CKF algorithm first act on the hyper-excitatory neural population 1, and then sequentially act on the nodes 7 and 5 with the highest degree. The modulation results are shown in Figure 19. The second specific pinning strategy is to first apply feedback control to the hyper-excitatory neural population 1, and then sequentially select nodes 7, 5 and 9 with the highest degree as the driving nodes. The modulation results are similar to which shown in Figure 19, so it is not repeated. It is not difficult to see from the figures that both strategies can quickly drive the spikes generated by the ''small-world'' neural population network to the expected alpha-like oscillations. The first random pinning strategy is to make the feedback control based on the fuzzy regulator and CKF algorithm act on nodes 1, 5 and 9, respectively, and the modulation results are shown in Figure 20. The second random pinning strategy is to exert the feedback control to neural populations 1, 3, and 4. The modulation results are similar to which shown in Figure 20, so it is not repeated. The third random pinning strategy not only applies feedback control to the hyper-excitatory neural population 1, but also randomly selects populations 3, 4 and 5 as the driving nodes, and the modulation results are shown in Figure 21. According

TABLE 4. Statistical data of the uniform distribution pinning control strategies.

Driving node set	Coupling strength	Control gain amplitude ("-" indicates negative feedback)	Control energy (mV)
{1,5,7}	30	$\lambda_1 = -13.57, \lambda_5 = -9.22, \lambda_7 = -11.43$	5.9045×10^5
	40	$\lambda_1 = -13.68, \lambda_5 = -13.68, \lambda_7 = -13.68$	8.6011×10^5
{1,5,7,9}	30	$\lambda_1 = -13.35, \lambda_5 = -8.62, \lambda_7 = -10.80, \lambda_9 = -8.40$	6.9806×10^5
	40	$\lambda_1 = -13.68, \lambda_5 = -11.00, \lambda_7 = -13.67, \lambda_9 = -10.03$	9.1276×10^5

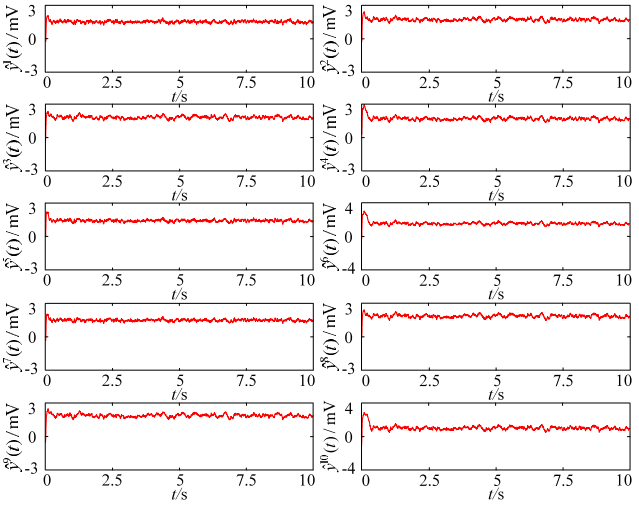

FIGURE 19. Modulation results of the first specific pinning strategy (1,5,7 are driving nodes).

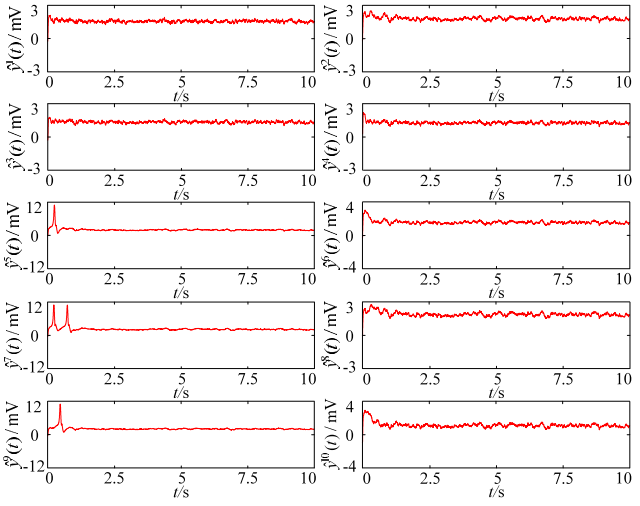

FIGURE 20. Modulation results of the first random pinning strategy (1,5,9 are driving nodes).

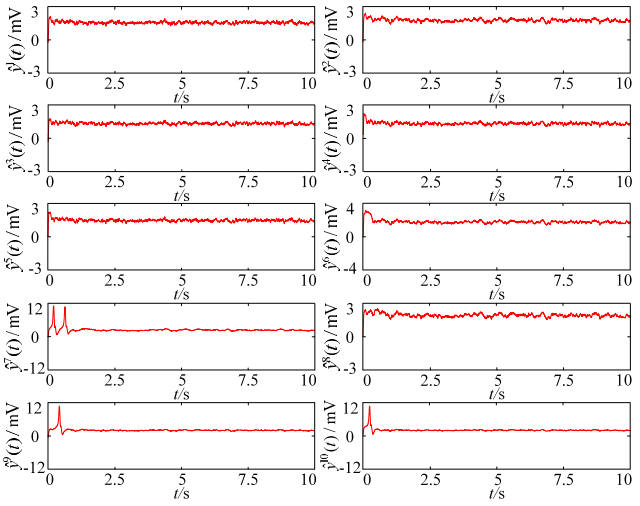

FIGURE 21. Modulation results of the first random pinning strategy (1,3,4,5 are driving nodes).

to these figures, it can be seen that the spikes generated by some nodes require a relatively obvious adjustment time before they are driven to the expected alpha-like oscillations. The above results indicate that the adjustment time required for achieving the modulation target using the specific pinning strategy is obviously shorter than that of the random pinning strategy. Therefore, the specific pinning strategy has significant advantages over the random pinning strategy when modulating the brain dynamics simulated by the ''small-world'' neural population network. We will then use the performance metric of the control cost to analyze the effectiveness of the more advantageous specific pinning strategy.

Table 4 presents statistical data for analyzing the effectiveness of the two proposed specific pinning strategies, where the values of control energy are calculated based on equation (9). It is not difficult to see from the table that: Firstly, when the coupling strength between neural populations is 30, the second strategy requires more control energy to achieve the modulation target compared to the first specific pinning strategy, but the control gain amplitudes required by driving nodes are relatively small; Secondly, for the first or second specific pinning strategy, with the increase of the coupling strength, the control energy required to achieve the modulation target increases, and the control gain amplitudes required by the driving nodes increase. These results indicate that the coupling strength and the number of driving nodes can affect the effectiveness of the specific pinning strategy for the ''small-world'' neural population network.

To sum up, the specific pinning strategy based on the fuzzy regulator and CKF algorithm has significant advantages over the random pinning strategy for the ''small-world'' neural population network whose output is affected by measurement noise. The statistical results further indicate that the coupling strength between neural populations and the number of driving nodes can affect the effectiveness of the specific pinning strategy. In general, for the ''small-world'' neural population network with a certain coupling strength, the specific pinning strategy with fewer driving nodes can better ensure the effectiveness when the control energy is required to be as small as possible; But when the feedback control gain

amplitudes of the driving nodes are required to be as small as possible, the specific pinning strategy with more driving nodes can better ensure the effectiveness. For a specific pinning strategy with a certain number of driving nodes, a smaller coupling strength between neural populations can better ensure its effectiveness, because the smaller the coupling strength, the less control energy and smaller control gain amplitudes are required to achieve the modulation target.

Additional Explanation: Firstly, for the neural population networks as shown in Figures 6, 7, 8, the increase of the coupling strength will lead to the generation and intensification of spikes. From this perspective, it is not difficult to understand the phenomenon that the control gain amplitudes and control energy required to achieve the modulation goal will increase with the increase of the coupling strength. Secondly, since the work considers that the large-scale spikes generated by networks are mainly triggered by a hyper-excitatory neural population, and the coupling strength between populations is maintained within a range that has a small impact on the network output, the spikes generated by the network will not be infinitely intensified, so the control gain amplitudes required by driving nodes will not be infinitely increased either.

IV. DISCUSSION

Neurostimulation has gradually become one of the most promising methods for treating neurological and psychiatric diseases due to its advantages of reversibility and small side effects [41], [42]. Considering the significant individual differences among patients with neurological and psychiatric diseases, it may be necessary to conduct extensive experiments to accurately select the stimulus position and determine the optimal stimulus intensity and other parameters. However, limitations in understanding the dynamic mechanisms of neural oscillations in direct animal and clinical trials, as well as immaturity of medical techniques and experimental conditions, may lead to irreversible brain injury and secondary damage. Mina et al. pointed out that control schemes developed based on neural computational models can simulate changes in brain dynamics under external stimulation [43]. Over the past few decades, two complementary neural computational models have been developed to simulate brain dynamics. Different from the FitzHugh-Nagumo model [44], Hidmarsh-Rose model [45], Hodgkin-Huxley model [46] and other neuron models that describe the activity of brain neurons at the cellular level, the neural population model that describes the activity of brain neuron populations at the level of cell set is both simple and more physiologically meaningful, balancing ease of processing and practicality, and more conducive to exploring the generation and evolution mechanisms of neural oscillations in depth. So the networks in the paper are constructed using the neural population model shown in equation (1) as nodes. We simulated the pathogenesis of neurological and psychiatric diseases by increasing the excitatory parameter of the first neural population. Under this condition, the established neural population network models generated abnormal neural oscillations with a large number of spikes. The output-feedback control scheme based on the fuzzy regulator and CKF algorithm was adopted to automatically adjust the control gain (used to predict the stimulus intensity), and different pinning control strategies (that help predict stimulus positions) were further adopted according to the degree distribution of nodes to simulate the response of brain dynamics to neurostimulation, which has a positive effect on predicting the optimal stimulus parameters for the treatment of neurological and psychiatric diseases caused by local hyper-excitatory brain regions.

From the perspective of complex network control theory, the design of local control schemes is an important aspect in solving the modulation problem of brain dynamics. It has been reported that the application of feedback strategies in epilepsy control can overcome the drawbacks that the selection of neurostimulation parameters depends entirely on the experience and level of the rehabilitation therapists. Its potential benefits include ensuring treatment effectiveness, improving response by providing intermittent or minimal stimulation, minimizing side effects, reducing damage, minimizing power consumption, and extending the battery life of implanted devices [47]. The basic requirement for implementing brain dynamics modulation through output-feedback control is that the output signal used to construct the control law can accurately reflect the functional state of the brain tissue [48]. However, the neural oscillation activity recorded by EEG, MEG, fMRI, LFP and other techniques may become inaccurate due to neuron and amplifier noise, as well as uncertain factors such as electrode resistance and capacitance in recording devices [49], so that the brain dynamic modulation system produces unexpected control behaviors. Therefore, it is of great significance to obtain useful information reflecting the actual activity state of the brain from the collected original data for designing output-feedback brain dynamic modulation systems. In addition, in view of the self-regulation characteristics of the brain system, if timely measures can be taken to suppress spikes and restore them to the brain self-regulation range as soon as possible (of course, the definition of this range is also one of the issues that urgently need to be solved by the majority of scientific research and medical personnel), which has a great potential to promote the restoration of normal brain function. That is to say, in addition to making the output of the controlled system track the expected alpha oscillation, suppressing spikes can also be used as the modulation target of the control system. The Schiff team first utilized the Unscented Kalman Filter (UKF) to estimate the actual output of the spatiotemporal model of the cerebral cortex from signals affected by measurement noise, and verified the superiority of the UKF based output-feedback control scheme in suppressing the abnormal activity of cortical neurons through numerical simulations [50]. The extended application of UKF based output-feedback control in the Hodgkin-Huxley

neuron model further demonstrates the feasibility of this approach in suppressing pathological brain activity, such as epilepsy [51]. Inspired by this, Liu and Gao designed an UKF based output-feedback control scheme to modulate the dynamics of the neural population model, thereby achieving the goal of suppressing persistent spikes [52]. Thus, for neural population network models whose output is affected by measurement noise, various nonlinear Kalman filter algorithms are the preferred algorithms for designing brain dynamic modulation schemes if the modulation target is to suppress spikes. Considering that the CKF exhibits better stability than the UKF in solving high-dimensional nonlinear problems, the work adopts CKF as the local controller. It has been confirmed that the fuzzy controller can be used as a regulator to adjust control parameters of the PID algorithm adaptively [53]. So we further introduced a fuzzy regulator into the local output-feedback control framework based on the CKF algorithm to adaptively adjust the control gain to ensure the modulation effect of brain dynamics.

Of course, it must be acknowledged that there are still some areas for improvement in the research work. 1) The models are still not perfect enough. Firstly, from the functional perspective, the perception and encoding of visual, auditory, and other signals by neurons in different regions of the cerebral cortex may need to be simulated by mathematical models with specific functions, rather than the universal neural population models; Secondly, neural population networks with 10 nodes still struggle to adequately describe the super complexity and high variability of the brain; Thirdly, the magnitude of coupling strength can affect the effectiveness of pinning control strategies, but we have not found selection rules for the coupling strength of neural population network models in existing references. In the paper, some coupling strengths that can ensure the effectiveness of pinning control strategies are selected through numerical simulations, which may not be very representative. Afterwards, we will attempt to construct a more realistic neural population network to simulate the generation and evolution mechanism of neural oscillations by modifying the differential equation form that describes the dynamic characteristics of neural populations, increasing the number of neural populations, and changing the coupling strength between neural populations. 2) The work has certain limitations in the hypothesis of the mechanism that triggers the onset of neurological and psychiatric diseases. Researches on human brain connectivity omics based on neuroimaging and electrophysiological techniques have shown that changes in the brain functional network connectivity may lead to the onset of neurological and psychiatric diseases. Liu et al. indicated that the ''small-world'' is the optimal connection mode for the brain functional network, and the disruption of this mode is the basis for the onset of schizophrenia [54]. The Stam team's research has demonstrated that the general feature of Alzheimer's patients is the loss of ''small-world'' characteristics in the brain functional network [55]. They also confirmed that patients exhibited significant randomization characteristics in their brain functional connectivity structures during seizures compared to normal individuals by analyzing the topological structure of brain functional networks in epilepsy patients [56]. Therefore, changes of structure characteristics in the brain functional networks are expected to become new indicators for diagnosing and monitoring the onset of neurological and psychiatric diseases. Obviously, under this assumption, research on network structure characteristics is crucial, and it is also necessary to take ''random'' neural population networks as the research object. 3) The research depth is insufficient. From the perspective of complex network control, it is very meaningful to determine the minimum number of nodes in the neural population network that require exerting external control. Taking the neural population networks such as ''nearest-neighbor'', ''scale-free'' and ''small-world'' as research objects, we will attempt to quantitatively calculate the minimum number of driving nodes required to achieve brain dynamic modulation targets under different topological structures using tools such as structural controllability theory and maximum matching principle in the future.

V. CONCLUSION

The paper proposes different pinning control strategies to modulate brain dynamics simulated by ''nearest-neighbor'', ''scale-free'' and ''small-world'' neural population networks whose outputs are affected by measurement noise. The simulation results show that, in addition to the need for the hyper-excitatory neural population to serve as a driving node, striving for a uniform distribution of driving nodes (uniform distribution pinning control method) can better ensure the effectiveness of the modulation strategy for the ''nearest-neighbor'' neural population network; selecting the nodes with the highest degree in networks in sequence as the driving nodes (specific pinning control method) can better ensure the effectiveness of modulation strategies for both ''scale-free'' and ''small-world'' neural population networks. Because these methods obviously require shorter adjustment time to achieve the modulation target of suppressing spikes. Meanwhile, statistical data further indicates that the number of driving nodes and coupling strength between neural populations not only affect the effectiveness of the uniform distribution and specific pinning control strategies, but also affect the control gain amplitude and control energy. For the ''nearest-neighbor'' neural population network, while ensuring the effectiveness of the uniform distribution pinning strategy, when the coupling strength is constant, the control energy will increase with the increase of the number of driving nodes, and control gain amplitudes will decrease with the increase of the number of driving nodes; when the number of driving nodes is constant, the control energy and control gain amplitudes will increase with the increase of the coupling strength. Therefore, for the ''nearest-neighbor'' neural population network with a certain coupling strength, the uniform distribution pinning strategy with fewer driving

nodes can better ensure effectiveness when the control energy is required to be as small as possible, but the uniform distribution pinning strategy with more driving nodes can better ensure effectiveness when the control gain amplitudes of driving nodes are required to be as small as possible. For the uniform distribution pinning strategy with a certain number of driving nodes, the effectiveness can be better ensured when the coupling strength between populations in the ''nearest-neighbor'' neural population network is relatively small. For the ''scale-free'' neural population network, while ensuring the effectiveness of the specific pinning strategy, when the coupling strength is constant, the control energy and control gain amplitudes will increase with the increase of the number of driving nodes; when the number of driving nodes is constant, the control energy and control gain amplitudes will increase with the increase of the coupling strength. Therefore, for the ''scale-free'' neural population network with a certain coupling strength, the specific pinning strategy with fewer driving nodes can better ensure effectiveness. For the specific pinning strategy with a certain number of driving nodes, the effectiveness can be better ensured when the coupling strength between populations in the ''scale-free'' neural population network is relatively small. For the ''small-world'' neural population network, while ensuring the effectiveness of the specific pinning strategy, when the coupling strength is constant, the control energy will increase with the increase of the number of driving nodes, and control gain amplitudes will decrease with the increase of the number of driving nodes; when the number of driving nodes is constant, the control energy and control gain amplitudes will increase with the increase of the coupling strength. Therefore, for the ''small-world'' neural population network with a certain coupling strength, the specific pinning strategy with fewer driving nodes can better ensure effectiveness when the control energy is required to be as small as possible, but the specific pinning strategy with more driving nodes can better ensure effectiveness when the control gain amplitudes of driving nodes are required to be as small as possible. For the specific pinning strategy with a certain number of driving nodes, the effectiveness can be better ensured when the coupling strength between populations in the ''small-world'' neural population network is relatively small.

CONFLICT OF INTEREST STATEMENT

The authors declare that the research was conducted in the absence of any commercial or financial relationships that could be construed as a potential conflict of interest.

REFERENCES

[1] S. Grillner, N. Ip, C. Koch, W. Koroshetz, H. Okano, M. Polachek, M.-M. Poo, and T. J. Sejnowski, ''Worldwide initiatives to advance brain research,'' *Nature Neurosci.*, vol. 19, no. 9, pp. 1118–1122, Aug. 2016, doi: 10.1038/nn.4371.

[2] L. Wang, ''Mu-ming poo: China brain project and the future of Chinese neuroscience,'' *Nat. Sci. Rev.*, vol. 4, no. 2, pp. 258–263, Feb. 2017, doi: 10.1093/nsr/nwx014.

[3] Y. Wang, J. Yin, G. Wang, P. Li, G. Bi, S. Li, X. Xia, J. Song, G. Pei, and J. C. Zheng, ''Responsibility and sustainability in brain science, technology, and neuroethics in China—A culture-oriented perspective,'' *Neuron*, vol. 101, no. 3, pp. 375–379, Feb. 2019, doi: 10.1016/j.neuron.2019.01.023.

[4] A. Fernandez-Ruiz, A. Sirota, V. Lopes-dos-Santos, and D. Dupret, ''Over and above frequency: Gamma oscillations as units of neural circuit operations,'' *Neuron*, vol. 111, no. 7, pp. 936–953, Apr. 2023, doi: 10.1016/j.neuron.2023.02.026.

[5] G. Buzsáki, *Rhythms of the Brain.* London, U.K.: Oxford Univ. Press, 2006.

[6] R. Traub and M. Whittington, *Cortical Oscillations in Health and Disease.* London, U.K.: Oxford Univ. Press, 2010.

[7] P. Hot, G. Rauchs, F. Bertran, P. Denise, B. Desgranges, P. Clochon, and F. Eustache, ''Changes in sleep theta rhythm are related to episodic memory impairment in early Alzheimer's disease,'' *Biol. Psychol.*, vol. 87, no. 3, pp. 334–339, Jul. 2011, doi: 10.1016/j.biopsycho.2011.04.002.

[8] V. K. Jirsa, W. C. Stacey, P. P. Quilichini, A. I. Ivanov, and C. Bernard, ''On the nature of seizure dynamics,'' *Brain*, vol. 137, no. 8, pp. 2210–2230, Aug. 2014, doi: 10.1093/brain/awu133.

[9] Z. Esmaeilpour, G. Kronberg, D. Reato, L. C. Parra, and M. Bikson, ''Temporal interference stimulation targets deep brain regions by modulating neural oscillations,'' *Brain Stimulation*, vol. 14, no. 1, pp. 55–65, Jan. 2021, doi: 10.1016/j.brs.2020.11.007.

[10] K. P. Michmizos, B. Lindqvist, S. Wong, E. L. Hargreaves, K. Psychas, G. D. Mitsis, S. F. Danish, and K. S. Nikita, ''Computational neuromodulation : Future challenges for deep brain stimulation [life sciences],'' *IEEE Signal Process. Mag.*, vol. 34, no. 2, pp. 114–119, Mar. 2017, doi: 10.1109/MSP.2016.2639554.

[11] J. Arle and J. Shils, *Innovative Neuromodulation: Neuromodulation for Psychiatric Disorders* New York, NY, USA: Academic, 2017.

[12] Z. Ma, ''Neurophysiological analysis of the genesis mechanism of EEG during the interictal and ictal periods using a multiple neural masses model,'' *Int. J. Neural Syst.*, vol. 28, no. 1, Feb. 2018, Art. no. 1750027, doi: 10.1142/s0129065717500277.

[13] T. Ying, A. N. Burkitt, and T. Kameneva, ''Combining the neural mass model and Hodgkin–Huxley formalism: Neuronal dynamics modelling,'' *Biomed. Signal Process. Control*, vol. 79, Jan. 2023, Art. no. 104026, doi: 10.1016/j.bspc.2022.104026.

[14] I. Basu, B. Crocker, K. Farnes, M. M. Robertson, A. C. Paulk, D. I. Vallejo, D. D. Dougherty, S. S. Cash, E. N. Eskandar, M. M. Kramer, and A. S. Widge, ''A neural mass model to predict electrical stimulation evoked responses in human and non-human primate brain,'' *J. Neural Eng.*, vol. 15, no. 6, Dec. 2018, Art. no. 066012, doi: 10.1088/1741-2552/aae136.

[15] O. David and K. J. Friston, ''A neural mass model for MEG/EEG:,'' *NeuroImage*, vol. 20, no. 3, pp. 1743–1755, Nov. 2003, doi: 10.1016/j.neuroimage.2003.07.015.

[16] P. J. Karoly, L. Kuhlmann, D. Soudry, D. B. Grayden, M. J. Cook, and D. R. Freestone, ''Seizure pathways: A model-based investigation,'' *PLOS Comput. Biol.*, vol. 14, no. 10, Oct. 2018, Art. no. e1006403, doi: 10.1371/journal.pcbi.1006403.

[17] M. Schirner, X. Kong, B. T. T. Yeo, G. Deco, and P. Ritter, ''Dynamic primitives of brain network interaction,'' *NeuroImage*, vol. 250, Apr. 2022, Art. no. 118928, doi: 10.1016/j.neuroimage.2022.118928.

[18] P. S. Goldman-Rakic and P. Rakic, ''Preface: Cerebral cortex has come of age,'' *Cerebral Cortex*, vol. 1, no. 1, pp. 1–10, Jan. 1991, doi: 10.1093/cercor/1.1.1-a.

[19] R. Salvador, J. Suckling, M. R. Coleman, J. D. Pickard, D. Menon, and E. Bullmore, ''Neurophysiological architecture of functional magnetic resonance images of human brain,'' *Cerebral Cortex*, vol. 15, no. 9, pp. 1332–1342, Sep. 2005, doi: 10.1093/cercor/bhi016.

[20] R. Salvador, J. Suckling, C. Schwarzbauer, and E. Bullmore, ''Undirected graphs of frequency-dependent functional connectivity in whole brain networks,'' *Phil. Trans. Roy. Soc. B, Biol. Sci.*, vol. 360, no. 1457, pp. 937–946, May 2005, doi: 10.1098/rstb.2005.1645.

[21] V. M. Eguíluz, D. R. Chialvo, G. A. Cecchi, M. Baliki, and A. V. Apkarian, ''Scale-free brain functional networks,'' *Phys. Rev. Lett.*, vol. 94, no. 1, Jan. 2005, Art. no. 018102, doi: 10.1103/physrevlett.94.018102.

[22] R. Ferri, F. Rundo, O. Bruni, M. G. Terzano, and C. J. Stam, ''Small-world network organization of functional connectivity of EEG slow-wave activity during sleep,'' *Clin. Neurophysiol.*, vol. 118, no. 2, pp. 449–456, Feb. 2007, doi: 10.1016/j.clinph.2006.10.021.

[23] S. Shirani, A. Valentin, B. Abdi-Sargezeh, G. Alarcon, and S. Sanei, "Localization of epileptic brain responses to single-pulse electrical stimulation by developing an adaptive iterative linearly constrained minimum variance beamformer," *Int. J. Neural Syst.*, vol. 33, no. 10, Aug. 2023, Art. no. 2350050, doi: 10.1142/s0129065723500508.

[24] L. Guo, H. Pan, and X. Nian, "Adaptive pinning control of cluster synchronization in complex networks with lurie-type nonlinear dynamics," *Neurocomputing*, vol. 182, pp. 294–303, Mar. 2016, doi: 10.1016/j.neucom.2015.12.024.

[25] O. J. Suarez, C. J. Vega, E. N. Sanchez, G. Chen, J. S. Elvira-Ceja, and D. I. Rodriguez, "Neural sliding-mode pinning control for output synchronization for uncertain general complex networks," *Automatica*, vol. 112, Feb. 2020, Art. no. 108694, doi: 10.1016/j.automatica.2019.108694.

[26] R. O. Grigoriev, M. C. Cross, and H. G. Schuster, "Pinning control of spatiotemporal chaos," *Phys. Rev. Lett.*, vol. 79, no. 15, pp. 2795–2798, Oct. 1997, doi: 10.1103/physrevlett.79.2795.

[27] F. M. Atay, T. Biyikoglu, and J. Jost, "Synchronization of networks with prescribed degree distributions," *IEEE Trans. Circuits Syst. I, Reg. Papers*, vol. 53, no. 1, pp. 92–98, Jan. 2006, doi: 10.1109/TCSI.2005.854604.

[28] H. Liu, X. Xu, J.-A. Lu, G. Chen, and Z. Zeng, "Optimizing pinning control of complex dynamical networks based on spectral properties of grounded Laplacian matrices," *IEEE Trans. Syst. Man, Cybern. Syst.*, vol. 51, no. 2, pp. 786–796, Feb. 2021, doi: 10.1109/TSMC.2018.2882620.

[29] T. Chen, X. Liu, and W. Lu, "Pinning complex networks by a single controller," *IEEE Trans. Circuits Syst. I, Reg. Papers*, vol. 54, no. 6, pp. 1317–1326, Jun. 2007, doi: 10.1109/TCSI.2007.895383.

[30] F. Wendling, J. J. Bellanger, F. Bartolomei, and P. Chauvel, "Relevance of nonlinear lumped-parameter models in the analysis of depth-EEG epileptic signals," *Biol. Cybern.*, vol. 83, no. 4, pp. 367–378, Sep. 2000, doi: 10.1007/s004220000160.

[31] X.-J. Li and G.-H. Yang, "Graph theory-based pinning synchronization of stochastic complex dynamical networks," *IEEE Trans. Neural Netw. Learn. Syst.*, vol. 28, no. 2, pp. 427–437, Feb. 2017, doi: 10.1109/TNNLS.2016.2515080.

[32] C. Hua, H. Wang, H. Wang, S. Lu, C. Liu, and S. M. Khalid, "A novel method of building functional brain network using deep learning algorithm with application in proficiency detection," *Int. J. Neural Syst.*, vol. 29, no. 1, Feb. 2019, Art. no. 1850015, doi: 10.1142/s0129065718500156.

[33] D. J. Watts and S. H. Strogatz, "Collective dynamics of 'small-world' networks," *Nature*, vol. 393, no. 6684, pp. 440–442, Jun. 1998, doi: 10.1038/30918.

[34] A.-L. Barabàsi and R. Albert, "Emergence of scaling in random networks," *Science*, vol. 286, no. 5439, pp. 509–512, Oct. 1999, doi: 10.1126/science.286.5439.509.

[35] A. López-Cuevas, B. Castillo-Toledo, L. Medina-Ceja, and C. Ventura-Mejía, "State and parameter estimation of a neural mass model from electrophysiological signals during the status epilepticus," *NeuroImage*, vol. 113, pp. 374–386, Jun. 2015, doi: 10.1016/j.neuroimage.2015.02.059.

[36] C. Sun, L. Geng, X. Liu, and Q. Gao, "Design of closed-loop control schemes based on the GA-PID and GA-RBF-PID algorithms for brain dynamic modulation," *Entropy*, vol. 25, no. 11, p. 1544, Nov. 2023, doi: 10.3390/e25111544.

[37] H. U. Voss, J. Timmer, and J. Kurths, "Nonlinear dynamical system identification from uncertain and indirect measurements," *Int. J. Bifurcation Chaos*, vol. 14, no. 6, pp. 1905–1933, Jun. 2004, doi: 10.1142/s0218127404010345.

[38] X. F. Wang and G. Chen, "Pinning control of scale-free dynamical networks," *Phys. A, Stat. Mech. Appl.*, vol. 310, nos. 3–4, pp. 521–531, Jul. 2002, doi: 10.1016/s0378-4371(02)00772-0.

[39] X. Li, X. Wang, and G. Chen, "Pinning a complex dynamical network to its equilibrium," *IEEE Trans. Circuits Syst. I, Reg. Papers*, vol. 51, no. 10, pp. 2074–2087, Oct. 2004, doi: 10.1109/TCSI.2004.835655.

[40] S. Li, D. Li, J. Wang, and H. Yu, "Iterative learning control algorithm for spiking behavior of neuron model," *Int. J. Modern Phys. B*, vol. 30, no. 1, Jan. 2016, Art. no. 1550240, doi: 10.1142/s0217979215502409.

[41] M. Parastarfeizabadi, R. V. Sillitoe, and A. Z. Kouzani, "Multi-disease deep brain stimulation," *IEEE Access*, vol. 8, pp. 216933–216947, 2020, doi: 10.1109/ACCESS.2020.3041942.

[42] C. Liu, G. Zhao, J. Wang, H. Wu, H. Li, C. Fietkiewicz, and K. A. Loparo, "Neural network-based closed-loop deep brain stimulation for modulation of pathological oscillation in Parkinson's disease," *IEEE Access*, vol. 8, pp. 161067–161079, 2020, doi: 10.1109/ACCESS.2020.3020429.

[43] F. Mina, P. Benquet, A. Pasnicu, A. Biraben, and F. Wendling, "Modulation of epileptic activity by deep brain stimulation: A model-based study of frequency-dependent effects," *Frontiers Comput. Neurosci.*, vol. 7, p. 94, Jul. 2013, doi: 10.3389/fncom.2013.00094.

[44] M. M. Ibrahim and I. H. Jung, "Complex synchronization of a ring-structured network of FitzHugh-Nagumo neurons with single- and dual-state gap junctions under ionic gates and external electrical disturbance," *IEEE Access*, vol. 7, pp. 57894–57906, 2019, doi: 10.1109/ACCESS.2019.2913872.

[45] Y. Xie, Y. Kang, Y. Liu, and Y. Wu, "Firing properties and synchronization rate in fractional-order Hindmarsh-Rose model neurons," *Sci. China Technol. Sci.*, vol. 57, no. 5, pp. 914–922, May 2014, doi: 10.1007/s11431-014-5531-3.

[46] X. Tang, Q. Zhang, X. Dai, and Y. Zou, "Neural membrane mutual coupling characterisation using entropy-based iterative learning identification," *IEEE Access*, vol. 8, pp. 205231–205243, 2020, doi: 10.1109/ACCESS.2020.3037816.

[47] S. Sunderam, B. Gluckman, D. Reato, and M. Bikson, "Toward rational design of electrical stimulation strategies for epilepsy control," *Epilepsy Behav.*, vol. 17, no. 1, pp. 6–22, Jan. 2010, doi: 10.1016/j.yebeh.2009.10.017.

[48] B. Shan, J. Wang, B. Deng, X. Wei, H. Yu, and H. Li, "UKF-based closed loop iterative learning control of epileptiform wave in a neural mass model," *Cognit. Neurodynamics*, vol. 9, no. 1, pp. 31–40, Aug. 2014, doi: 10.1007/s11571-014-9306-0.

[49] B. Deng, J. Wang, and Y. Che, "A combined method to estimate parameters of neuron from a heavily noise-corrupted time series of active potential," *Chaos, Interdiscipl. J. Nonlinear Sci.*, vol. 19, no. 1, Mar. 2009, Art. no. 015105, doi: 10.1063/1.3092907.

[50] S. J. Schiff and T. Sauer, "Kalman filter control of a model of spatiotemporal cortical dynamics," *BMC Neurosci.*, vol. 9, no. S1, pp. 1–8, Jul. 2008, doi: 10.1186/1471-2202-9-s1-o1.

[51] G. Ullah and S. J. Schiff, "Tracking and control of neuronal Hodgkin–Huxley dynamics," *Phys. Rev. E, Stat. Phys. Plasmas Fluids Relat. Interdiscip. Top.*, vol. 79, no. 4, Apr. 2009, Art. no. 040901, doi: 10.1103/physreve.79.040901.

[52] X. Liu and Q. Gao, "Parameter estimation and control for a neural mass model based on the unscented Kalman filter," *Phys. Rev. E, Stat. Phys. Plasmas Fluids Relat. Interdiscip. Top.*, vol. 88, no. 4, Oct. 2013, Art. no. 042905, doi: 10.1103/physreve.88.042905.

[53] X. Liu, H. Liu, Y. Tang, and Q. Gao, "Fuzzy PID control of epileptiform spikes in a neural mass model," *Nonlinear Dyn.*, vol. 71, nos. 1–2, pp. 13–23, Oct. 2012, doi: 10.1007/s11071-012-0638-1.

[54] Y. Liu, M. Liang, Y. Zhou, Y. He, Y. Hao, M. Song, C. Yu, H. Liu, Z. Liu, and T. Jiang, "Disrupted small-world networks in schizophrenia," *Brain*, vol. 131, no. 4, pp. 945–961, Feb. 2008, doi: 10.1093/brain/awn018.

[55] E. J. Sanz-Arigita, M. M. Schoonheim, J. S. Damoiseaux, S. A. R. B. Rombouts, E. Maris, F. Barkhof, P. Scheltens, and C. J. Stam, "Loss of 'small-world' networks in Alzheimer's disease: Graph analysis of fMRI resting-state functional connectivity," *PLoS ONE*, vol. 5, no. 11, Nov. 2010, Art. no. e13788, doi: 10.1371/journal.pone.0013788.

[56] S. C. Ponten, F. Bartolomei, and C. J. Stam, "Small-world networks and epilepsy: Graph theoretical analysis of intracerebrally recorded mesial temporal lobe seizures," *Clin. Neurophysiol.*, vol. 118, no. 4, pp. 918–927, Apr. 2007, doi: 10.1016/j.clinph.2006.12.002.

CHENGXIA SUN received the B.S. degree in electrical engineering and automation and the Ph.D. degree in control science and engineering from Yanshan University, China, in 2015 and 2021, respectively. Since 2021, she has been a Lecturer with the Mechanical and Electrical Engineering College, Hebei Normal University of Science and Technology, China. Her research interests include mechanism for neural oscillation, modulation of neural oscillation, control theory, and complex network theory.

LIJUN GENG received the B.S. degree in electrical engineering and automation and the Ph.D. degree in power system and automation from Yanshan University, China, in 2015 and 2021, respectively. Since 2021, she has been a Lecturer with the Mechanical and Electrical Engineering College, Hebei Normal University of Science and Technology, China. Her research interests include applied optimization and energy economics, coupled transportation, and power distribution systems.

HONGJU LIN received the B.S. degree in computer and application from Jilin University, Changchun, Jilin, China, in 2000, the M.S. degree in power electronic and electrical drive from Xihua University, Chengdu, Sichuan, China, in 2005, and the Ph.D. degree in instrument science and technology from Yanshan University, Qinhuangdao, Hebei, China, in 2018. From 1999 to 2002, he was an Assistant Engineer with Harbin Electric Machinery Company Ltd. Since 2005, he has been a Lecturer, an Associate Professor, and a Professor with the School of Mechanical and Electrical Engineering, Hebei Normal University of Science and Technology, Qinhuangdao. He is the author of more than 30 articles. His research interests include network control technology and system simulation.

YUQUAN MA was born in January 1971. He received the bachelor's degree in electric machines from Xi'an Jiaotong University, in July 1993, and the master's degree in high voltage and insulation technology from Hebei University of Technology, in June 2009. Since 2002, he has been a Professor with Mechanical and Electrical Engineering College, Hebei Normal University of Science and Technology, China. His research interest includes electrical control engineering and has presided over a technological innovation project, DCS-based hardware-in-the-loop simulation system for safe operation of styrene plants, suppported by medium-sized scientific and technological enterprises in Hebei.

XIAN LIU received the Ph.D. degree in general mechanical and basics mechanics from Peking University, Beijing, China, in 2008. Since 2015, she has been a Professor with the Institute of Electrical Engineering, Yanshan University, China. She was an Academic Scholar with the Department of Psychiatry, University of Cambridge, U.K., in 2022. Her research interests include mechanism for neural oscillation, modulation of neural oscillation, control theory, and complex network theory.

JIANJIANG LI was born in Tangshan, Hebei, in May 1976. He received the bachelor's degree in safety engineering in the field of engineering technology from Harbin University of Science and Technology, in 2001, and the master's degree in business administration from Beijing University of Aeronautics and Astronautics, Beijing, China, in 2018. Since 2009, he has been the Executive Director of Tangshan Shangxinrongda Electronic Products Company Ltd. He is currently the Director of the Provincial Innovation Center and Provincial Enterprise Technology Center of Hebei Province.